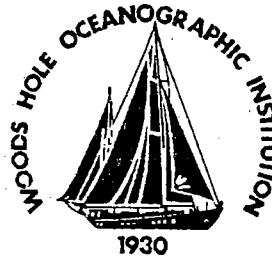# Woods Hole Oceanographic Institution

1930

Smoothly Modulated Frequency-Bounded Impulse Signals for Tomography
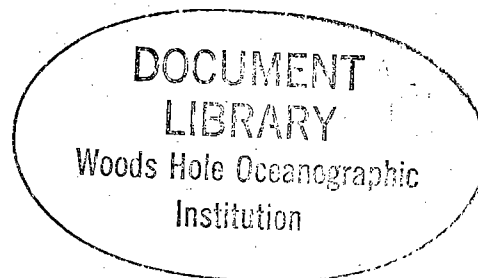
by

Timothy F. Duda and James F. Lynch

June 1991

Technical Report

WHOI-91-13

Smoothly Modulated Frequency-Bounded Impulse Signals for Tomography

by

Timothy F. Duda and James F. Lynch

Woods Hole Oceanographic Institution
Woods Hole, Massachusetts 02543

June 1991

Technical Report

Approved for Distribution:

Albert J. Williams 3rd

Albert J. Williams 3rd, Chairman
Department of Applied Ocean Physics
and Engineering

Abstract:

A group of amplitude and frequency modulated signals which generate narrow synthesized pulses and which also have smoothly varying phase are described. The frequency-sweep (chirp) signals have exactly-defined frequency content and differentiable phase. These signals can be used with efficient resonant transducers, if the resonant frequency is adjustable, and they have adequate Doppler response for use with drifting apparatus.

1. Introduction

In the 1980's and early 1990's ocean acoustic tomography experiments, which use pulse travel-time measurements to create sound-speed maps, have used phase modulation pulse compression techniques [1]. A carrier was phase modulated with special pseudorandom codes (M-sequences), which have single-spike, two-valued autocorrelation functions. After reception, cross-correlation of the signals with the transmitted signal (matched filtering) yielded high travel-time resolution. The only shortcoming of this technique, which is optimized in numerous ways [2], is that transducers in general can not make instantaneous phase transitions, so that only approximations to the ideal signals are actually possible. Since the ideal M-sequence signals can not possibly be transmitted, we evaluate the performance of less optimal pulse compression techniques which can be more accurately transferred from theory to experiment. In particular, we will show properties of linear frequency sweep signals, amplitude modulated with smooth functions, which we call AM-FM signals.

2. Spectra of Synthetic Pulse Signals

The power spectrum of the transmitted signal is fundamentally related to the achievable time resolution. The optimal temporal response, the delta function, corresponds to a signal with a uniform power spectrum. The M-sequence signals, which have specific digit lengths corresponding to a small number of carrier cycles, have sinc^2 power spectra, the same spectra as rectangular pulses (digital pulses, in a sense). Figure 1 shows the power spectra of M-sequence phase-modulated signals, with two modulation angles. The power spectra are the sums of the sinc^2 spectrum and the line spectrum of the carrier. In the pulse-synthesis scheme, the correlation process (in the time domain) can be treated in the frequency domain as multiplication of the received signal spectrum and the complex conjugate of the transmitted signal, so that the matched-filter outputs are equal to Fourier transforms of squares of the transmitted signal spectrum. For the M-sequence example, the sinc^4 spectral product of the filtering procedure yields a triangular matched filter output. A residual mean level results from the carrier energy and is a function of the modulation angle.

Figure 2a shows the spectrum of an M-sequence code with a shorter 3-cycle digit, with better temporal resolution that the 4-cycle/digit codes of Fig. 1. Figure 2b shows the spectrum of a tenth-order butterworth bandpassed version of the same signal, simulating the filtering effect of a transducer. After matched-filter processing, the synthetic output pulse is widened for the filtered version of the signal, as expected (Figure 3). Side lobes also result from the limited bandwidth. Examples of this effect can be seen in experimental data.

Figure 4 shows a time-lagged autocovariance function of a sharp-processed M-sequence signal from the Slice89 Experiment [3]. The sharp-processing matched-filter [4], utilized for speed, gives a boxcar output, instead of a triangle, so that an auto-correlation of the ideal synthetic pulse would yield the indicated triangle, similar to the true matched filter. The similarity of Figures 3 and 4 is due in part to the limited bandwidth of the Slice89 transmission, and in part to the 1000-km propagation.

Because the M-sequences have the optimum time resolution of any codes, they have the most energetic sidelobes and therefore are least-faithfully reproduced by apparatus. The truncation of the sidelobes arises from the inability of the transducer to make instantaneous phase transitions, and limits the usefulness of the optimal codes. Two difficulties also arise from use of the M-sequences. One is the requirement of low Q, non resonant transducers, with no potential for efficiency gain through resonance. The second difficulty is the extreme sensitivity of the M-sequence to Doppler shifts.

Since the ideal nature of the M-sequences cannot be utilized due to limited bandwidths, the other two sacrifices seem a high price to pay for their use. We investigate here a class of amplitude and frequency modulated signals which do not force these sacrifices. The essential idea is that one does not attempt to transmit the sidelobes, but tapers the frequency content such that the temporal response is improved [5]. The price one pays, through amplitude modulation, is the lower total power in the signals, so that more time is required to achieve the same gain. This is an important consideration in a rapidly fluctuating ocean environment.
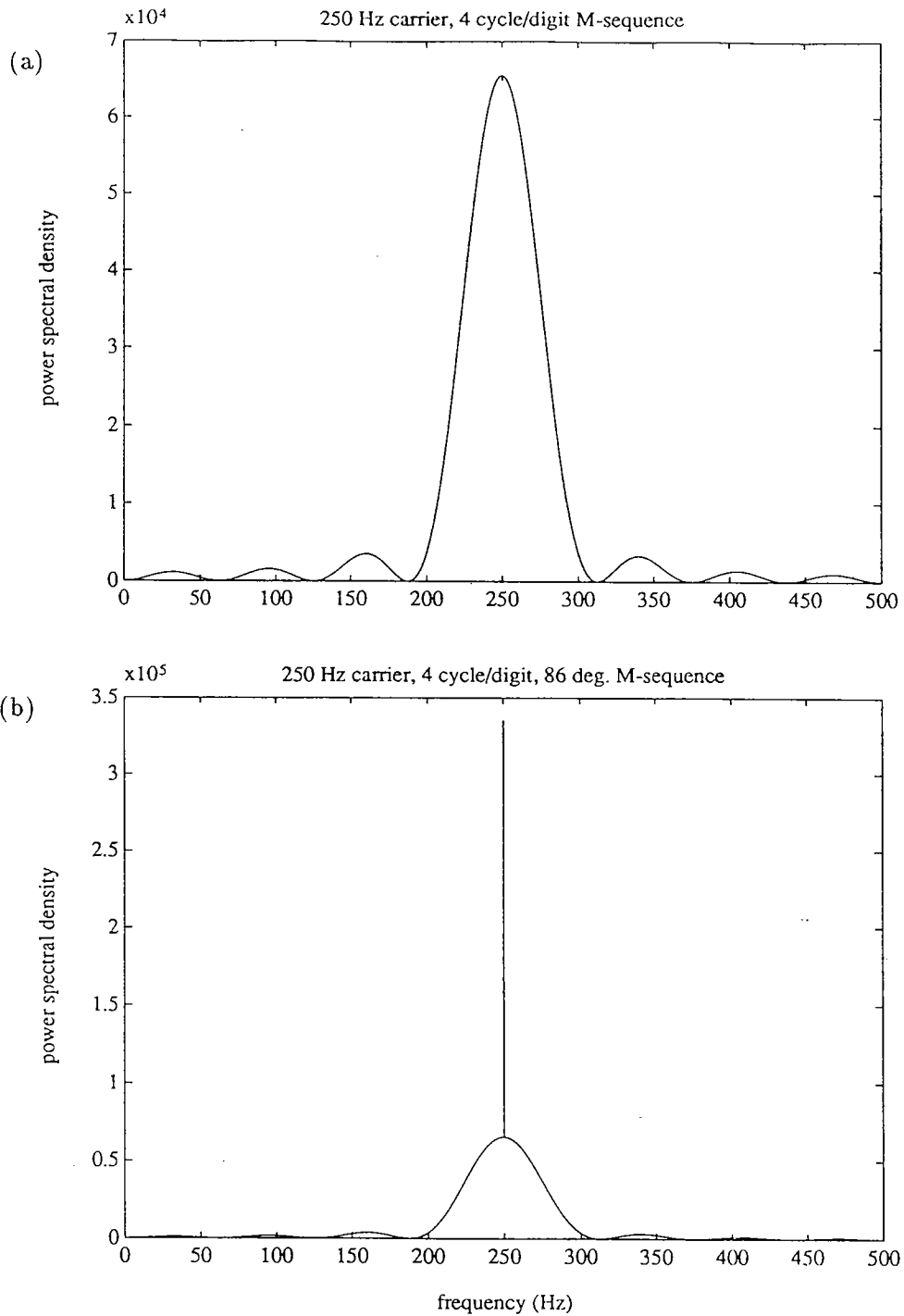
4

Figure 1. These are power spectrum of M-sequence phase modulated signals with 1023 digits and 4 cycles of a 250 Hz carrier per digit. Frame (a) shows the smooth sinc squared envelope one gets if the modulation angle is $\tan^{-1}(\sqrt{(1023)})$, about 88.2 degrees, while (b) shows the result for 86 degree modulation. The extra carrier will produce a DC component in the matched filter.
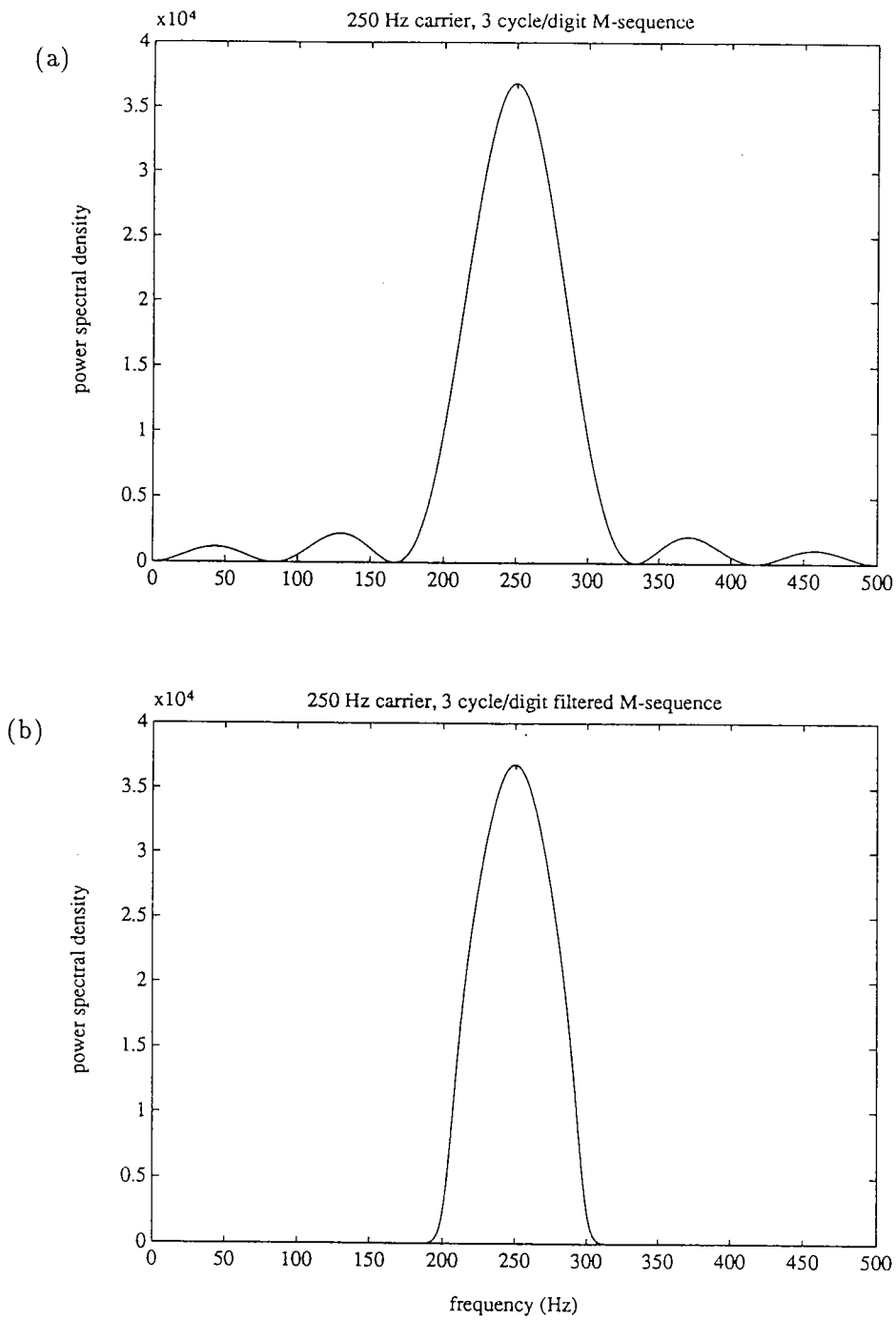
Figure 2. Power spectra of unfiltered (a) and filtered (b) versions of a phase-modulated, 3 cycle/digit, 250 Hz carrier M-sequence signal. A tenth-order bandpass butterworth filter is employed.
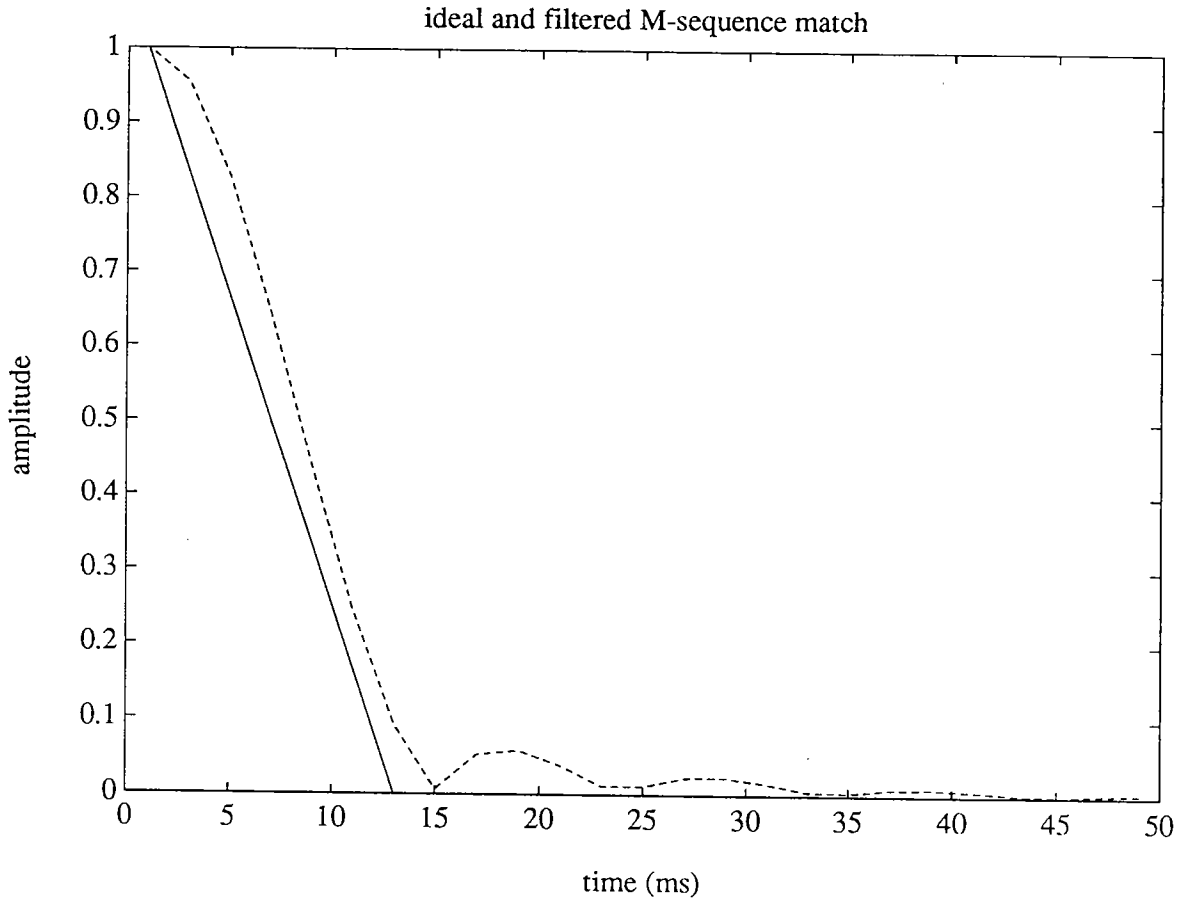
Figure 3. Shown are one-half side of the matched filter outputs for the ideal and filtered M-sequence phase-modulated signals, whose spectra are seen in Figure 2. The truncation of frequencies gives the side-peaks.

3. Spectral Control using Amplitude Modulation

Since frequency is the time derivative of phase, analytic descriptions of phase conveniently describe frequency modulation. This makes for a more compact signal description than for the M-sequences. We concentrate on linear frequency-sweep signals, with phase following the square of time (plus an additional term concerning the center frequency):

$$s(t) = A(t)e^{i\theta(t)} \quad ; \qquad \theta(t) = \frac{bt^2}{2} + \omega_o t$$

Amplitude modulation over time can be used to precisely control frequency content, since frequency is a function of time $(f(t) = bt + \omega_o)$. The spectral density follows the inverse formula $S(f) = A(g(f))$, where $g(f) = (f - \omega_o)/b$ is the inverse function of $f(t)$. Since g is a linear function of frequency, the spectral density $S(f)$ follows the form $A(t)$, with scaling.

We will use the spectral estimation tapers for A, since they will have the desired frequency content and will reduce the matched-filter sidelobes [6]. The first example is cosine-taper modulation, $A(t) = \cos^n(t)$. The case $n = 2$ is also called the Hanning taper. In the absence of noise or Doppler shifts, the frequency rate-of-change b (or the total transmission time) is not important, only the total range of frequencies. A 120-Hz band is used, like that of the M-sequence example (Figure 2b). Figure 5 shows synthetic pulse shapes (match-filter) for $n = 1, 2, 3$, and for boxcar modulation, $A(t)$ fixed over the transmission duration (i.e. fixed over frequency). Since different tapers result in different transmitted power, match-filter outputs are normalized by transmitted power. The matched filtering involves the squaring of the frequency response $S(f)$, so that the $n = 1$ modulation scheme gives a pulse shape equal to the transform of the Hanning window ($n = 2$), and so on. This has no effect for the boxcar, so that the boxcar produces a sinc^2 pulse.

The boxcar produces the narrowest peak and the highest sidelobes, as expected. The distribution of energy over the available band gives the narrowness of the peak, but the sharp cutoff produces the ringing effect. The cosine^n tapers reduce the sidelobes, but broaden the peak considerably. The cosine windows are often used since they are simple analytic forms, and do reduce

8

sidelobe leakage, but they are not optimal. There are many window families which reduce sidelobes with less widening of the main lobe.

The functions which have the highest ratio of main-lobe to side-lobe energy, for a given peak width, are the prolate spheroidal functions [6,7]. For convenience we consider the slightly less optimal Chebyshev tapers, which are available in the MATLAB signal-processing software package. That program will calculate Chebyshev tapers with any desired sidelobe level [8]. To create synthetic pulses with the known sidelobe characteristics of the Chebyshev windows, one can use amplitude functions $A(t)$ following the square-root of Chebyshev windows. Figure 6 shows synthetic pulse (matched-filter) output for seven Chebyshev windows with maximum sidelobes of -14 to -32 dB. These maximum sidelobes are roughly equivalent to the noise level for 1000 km ocean transmission with typical radiators and 2-minute codes. The main lobes are not quite as narrow as the ideal M-sequence (Fig. 3) or the boxcar transmission (Fig. 5), but are similar to the degraded M-sequence (Fig. 3). Therefore, careful choice of amplitude modulation can reproduce the performance of the M-sequences with less signal complexity.

4. Doppler Response

If there exists a non-zero relative velocity between source and receiver, a received signal will appear as though it were received with a compressed or stretched time scale, relative to the zero-velocity case. For small velocity, a good approximation to the total length of the reception is

$$T_d = T[1 - v/c]$$

where c the wave speed, $v \ll c$ is the relative closing velocity, and T the duration of the transmission. In the cw case, since the same number of waves is received as transmitted, it is clear that the frequency shift is near

$$\omega_d = \omega[1 + v/c]$$

The effect on signal coherence is clear if one considers the difference between $s(t - vt/c)$ and $s(t)$. At the total duration T, the signal mismatch is maximum. Conventionally, it is argued that a
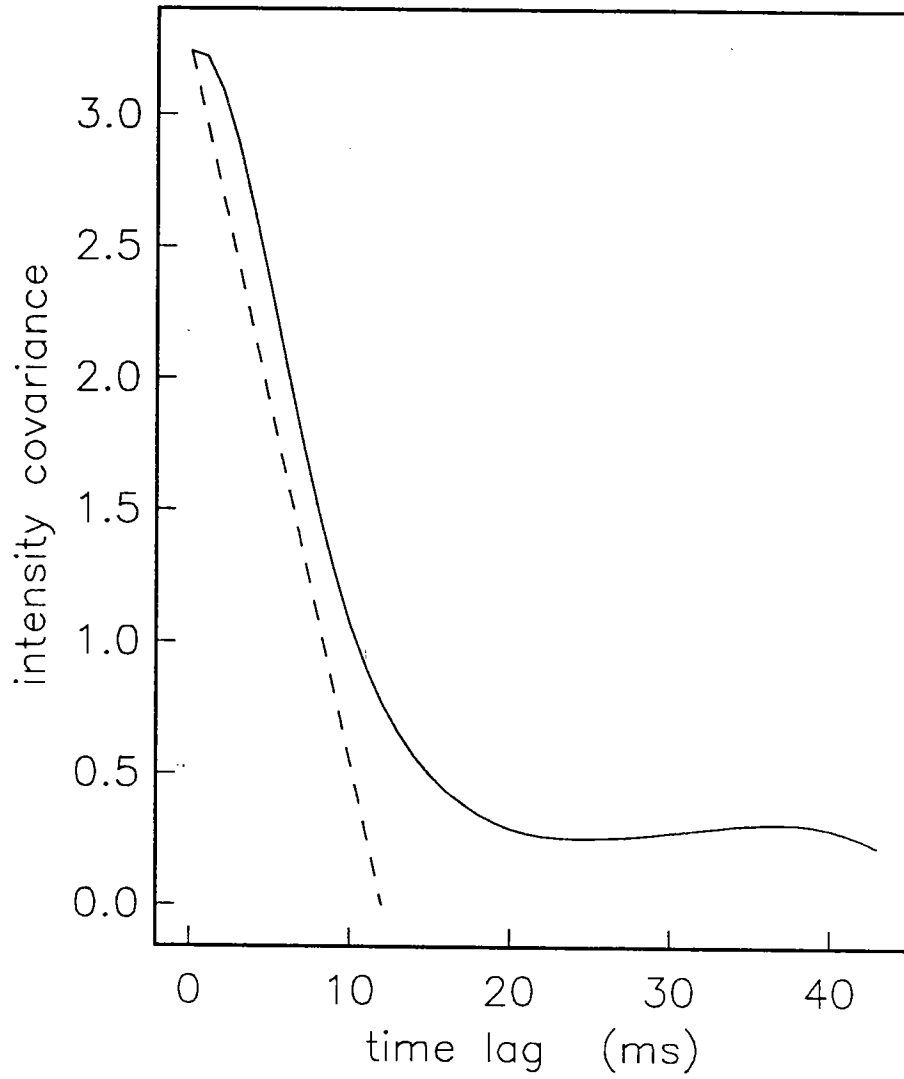
9

Figure 4. The autocovariance function of the square of a single example of the matched-filter output of the slice89 experiment, which is wider than the ideal output (the ramp) and similar to the simulation of Figure 3.
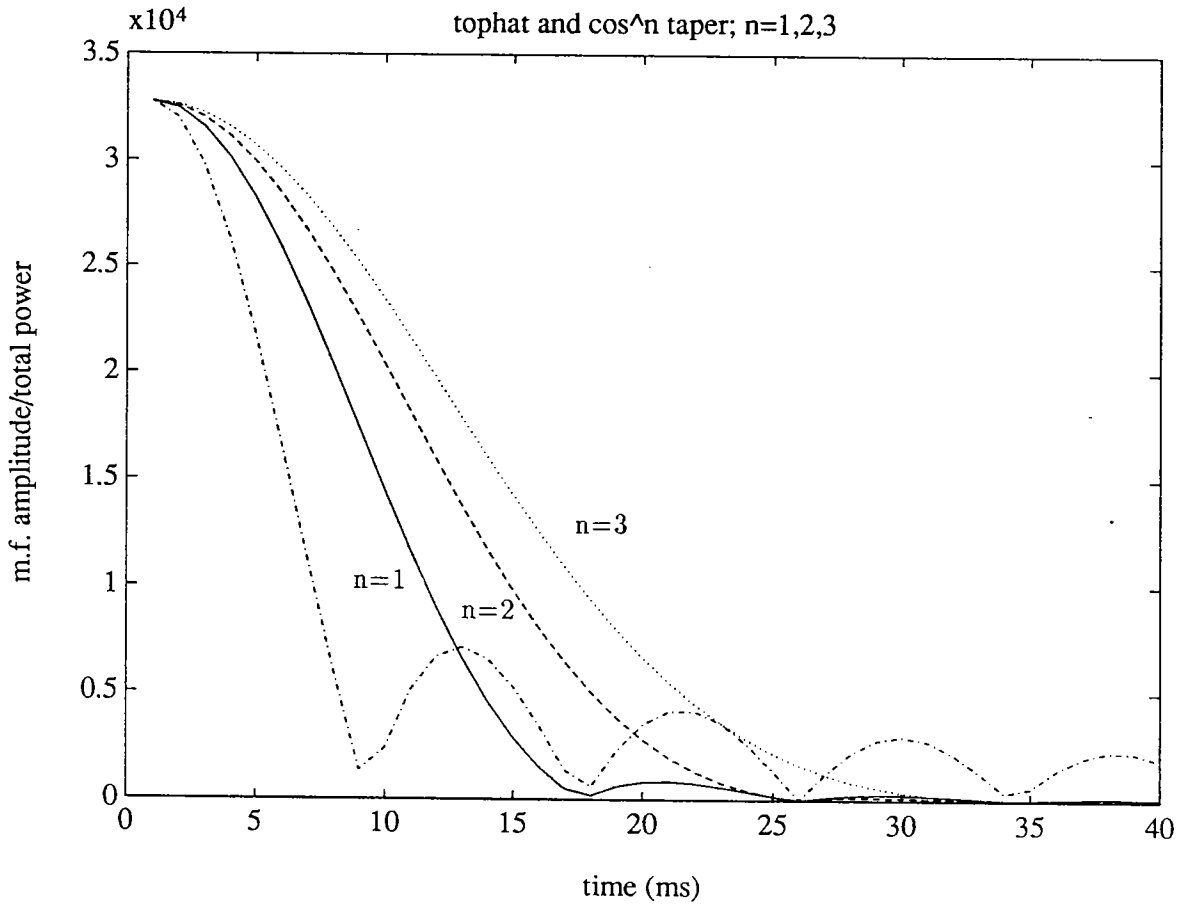
Figure 5. Matched-filter outputs for various taper functions $A(t)$. The total swept band is 120 Hz. The narrowest main peak is produced by the boxcar function (no amplitude modulation). The solid line is the result of cosine tapering, the dashed from $\cos^2$, and the dotted (widest peak) is from $\cos^3$ tapering.
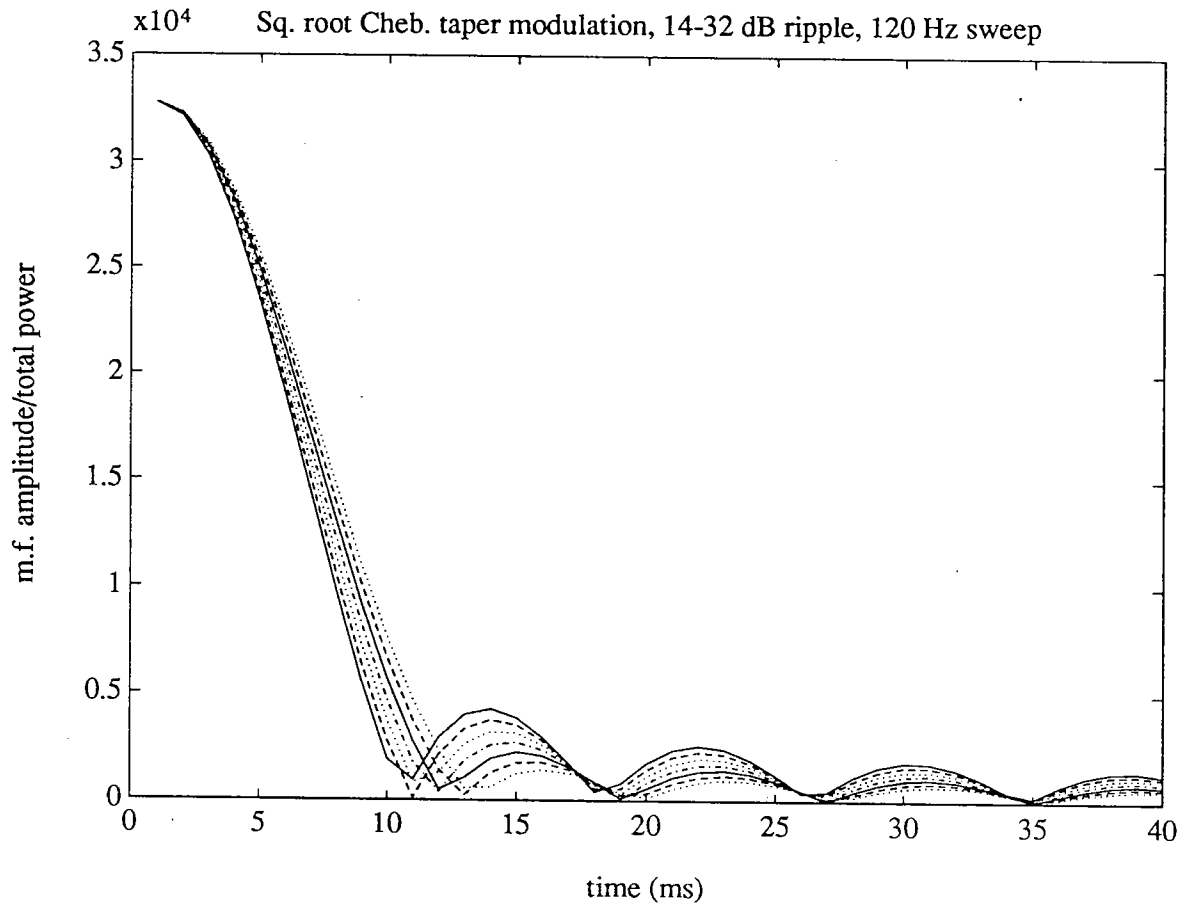
11

Figure 6. Matched filter outputs using Chebyshev taper signals over a 120 Hz swept band. A continuous choice of main peak width vs. side peak size is available. The performance is better than the cosine tapers, with a distribution of energy into many small sidelobes allowing a narrower main peak.

signal with bandwidth W cannot change much in time W^{-1}, so that Doppler effects are minimal if [9]

$$\frac{vT}{c} \ll W^{-1}$$

or

$$WT \ll \frac{c}{v}$$

This time-bandwidth product criterion is very stringent for typical ocean tomographic transmissions, which must be long to achieve gain. M-sequence codes of 120 s duration and 83 Hz bandwidth loose coherence at about $v = 0.05$ m/s, or 0.1 knots Doppler. The lost coherence results in great attenuation of the matched filter output. The mismatch of the precise pattern of digits is responsible for the incoherence.

The smooth phase (or frequency) variations of the amplitude-modulated linear frequency sweep signals give increased coherence between a compressed reception and a non-compressed replica. This is because the frequency sweep rate is changed only slightly and the amplitude modulation is smooth. The result is performance in excess of the WT product criterion. Figure 7 shows the Doppler performance for a 120 s, 120 Hz, amplitude-modulated frequency up-sweep. The widened peak is quite good at 0.5 m/s Doppler, and still usable at 1 m/s. The "toward", or "blue" Doppler shift is indicated by the progressive time shift of the peak. A down sweep would have an opposite time shift. Also shown in Figure 7 is the relative loss of gain vs. closing velocity.

The AM-FM signals have increased Doppler performance over boxcar (no AM) linear FM sweeps. In the previous section the large sidelobes of the boxcar linear FM sweep were shown to be large, and Figure 8 shows how they degrade the Doppler performance relative to the AM-FM signals. The broad multiple nature of the peaks is unacceptable, and the AM-FM signals appear to have optimal Doppler performance as well as optimally narrow matched-filter response.
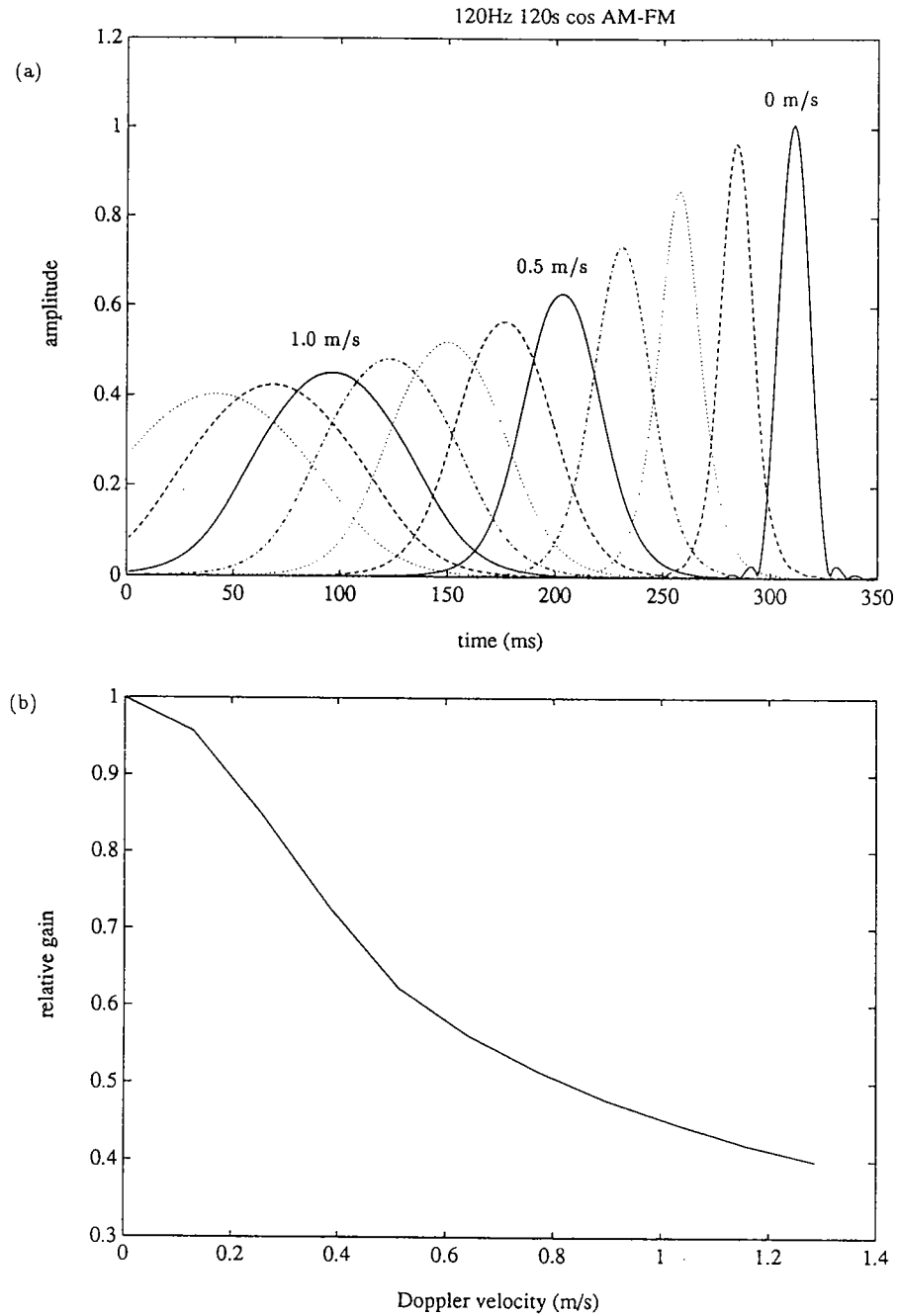
Figure 7. (a) Synthetic pulse (matched filter) results of a relative source-receiver motion simulation using a two minute, 120 Hz band cosine AM-FM signal. The step in velocity v is 0.125 m/s, from 0 to 1.25 m/s. A two minute M-sequence signal would produce only a large $v = 0$ peak and a small $v = 0.125$ m/s peak, while gives wide but visible peaks to over 1 m/s. Frame (b) shows the peaks heights from frame (a), relative to the $v = 0$ case.
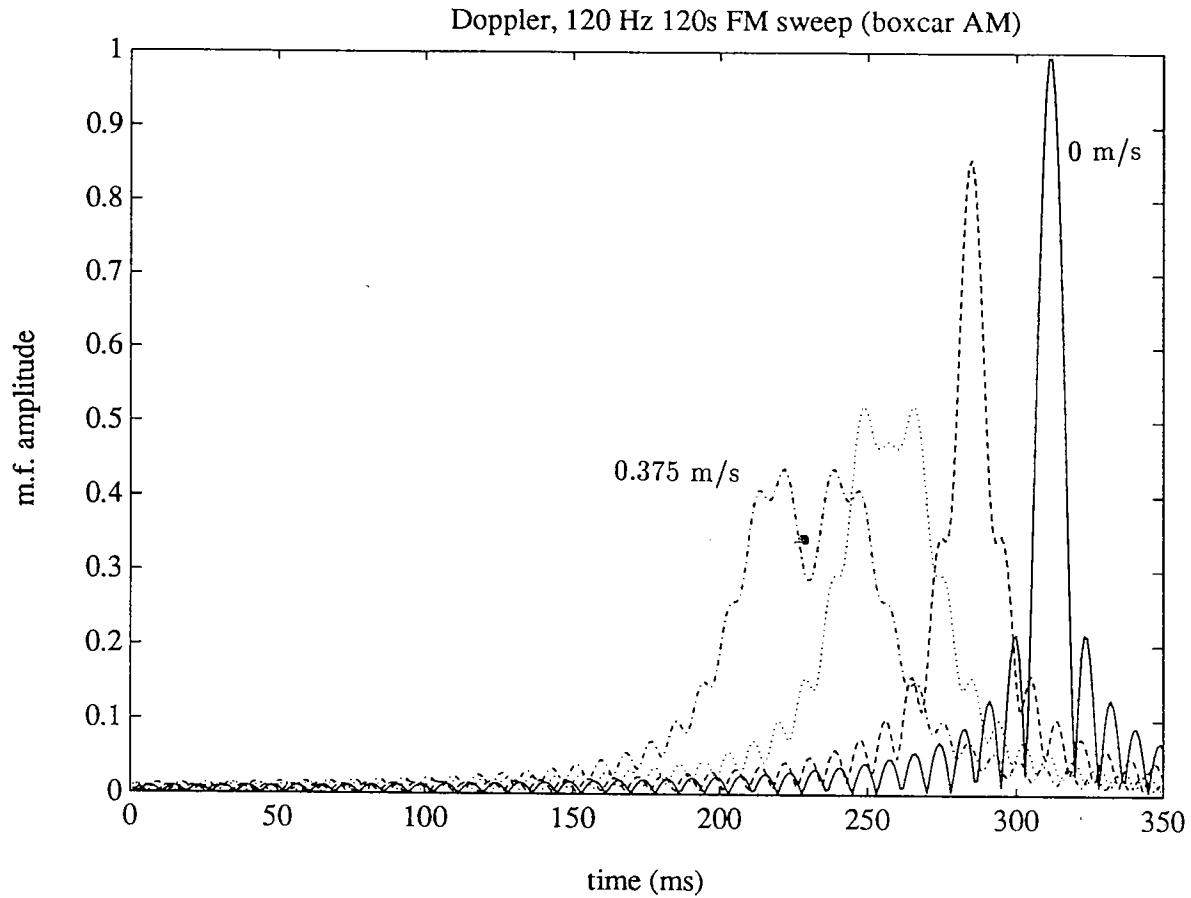
Doppler, 120 Hz 120s FM sweep (boxcar AM)

Figure 8. With source/receiver motion, the performance of the FM only linear sweep (boxcar AM) is inferior to that of the AM-FM signal. The velocity step is the same as Figure 7. A double peak appears at $v = 0.25$ m/s, with very poor performance at greater v.
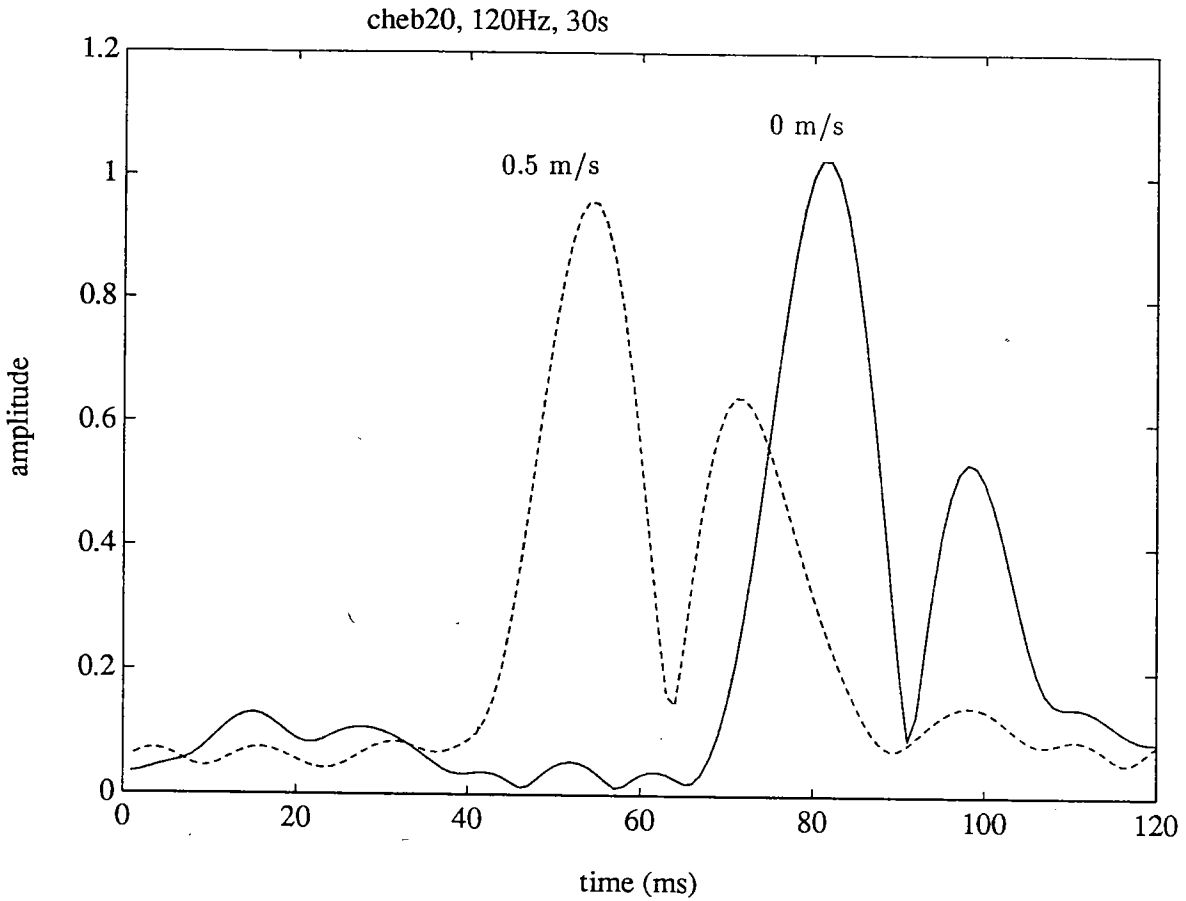
Figure 9. Synthetic multipath pulse results are very encouraging with both high noise (*SNR* of -20 dB) and high relative source-receiver velocity. Two simulated arrivals at two Doppler velocities (0 and 0.5 m/s) are shown. A -20 dB ripple Chebyshev window is employed. The peaks, arriving at 80 and 98 ms, are easily distinguished, with the early arrival shift apparent in the non-zero Doppler case. The amplitude variation from the noise masks the slight peak attenuation from the Doppler shift, shown in the noiseless Fig. 7a case.

cheb20, 120Hz, 30s

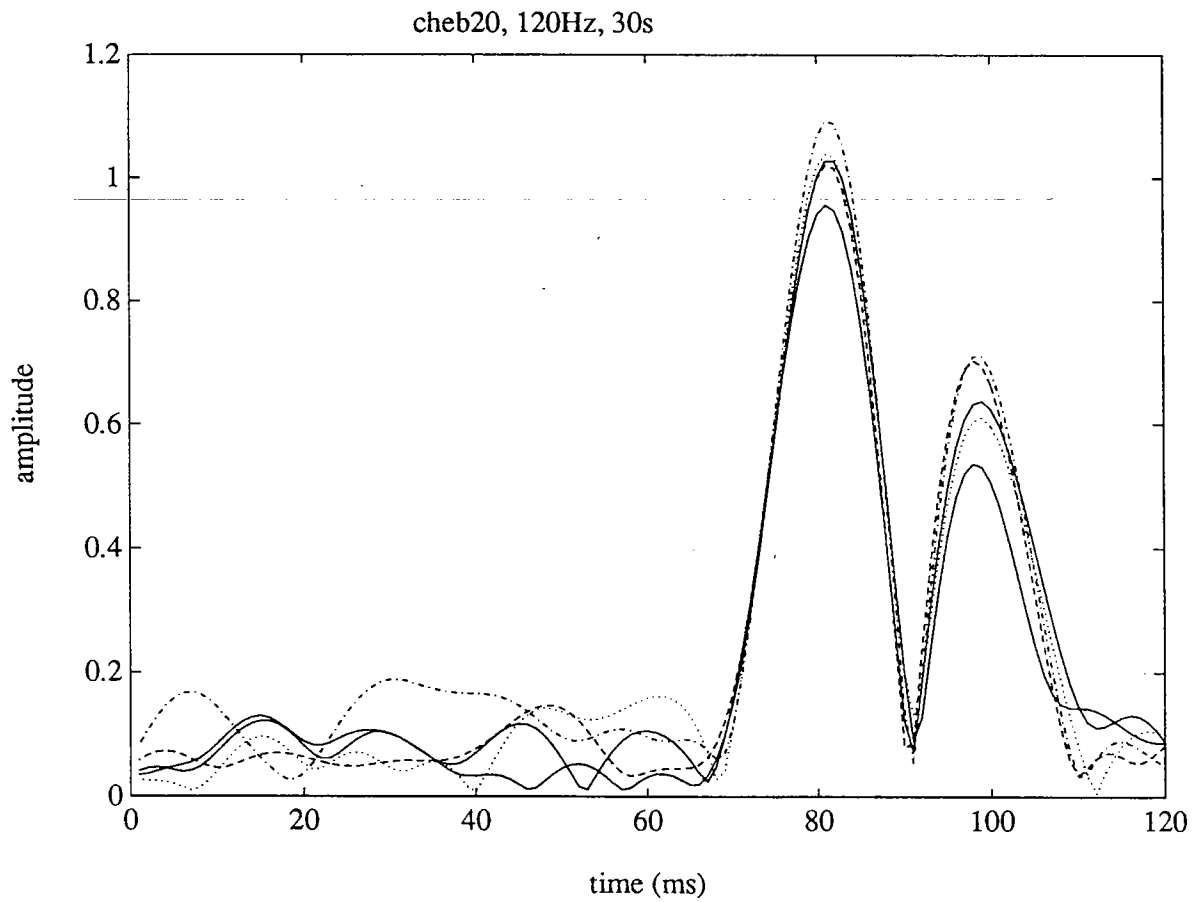Figure 10. Repeated simulations of 30 second AM-FM pulse synthesis with signal/noise ratio of -20 dB show some variability in the peak height. Results of five runs are shown, the difference in the runs being solely in the gaussian random noise component. A -20 dB Chebyshev taper is used.

5. Summary

A family of frequency sweep signals with tapered attenuation at the ends of the band can be used to synthesize pulses with both a narrow main peak and low side peaks. The shapes of the main and side peaks are controlled by the tapering, also called the amplitude modulation. A broad range of taper functions can be used in this AM-FM scheme, depending upon signal/noise ratio, expected peak spacing, etc., in order to optimize the signal. The best taper functions to use are the spectral estimation taper functions, which have optimum properties for this operation. Tapering with the square root of the desired taper function will reproduce a pulse shaped like the Fourier transform of the taper. If the frequency response of the system can be measured, this can be applied to the taper to optimize the output, that is, the applied taper can be adjusted so that the final transmitted spectrum has the desired shape. In theory, one can utilize the entire frequency range of any equipment, so that the peak resolution attainable with pseudorandom M-sequences can be achieved.

The AM-FM linear frequency sweep signals give enhanced Doppler performance over simple linear FM sweeps, which in turn give better performance than the pseudorandom phase modulation scheme. The gain in the presense of relative source-receiver motion of the (linear) FM chirp signal is retained by the AM-FM chirp, but the multiple peak problem of the FM signal is greatly reduced.

To illustrate the usefulness, a test run with a 30 second sweep and -20 dB signal/noise ratio (ratio of signal power/noise power of 0.01) was performed (Figure 9). Two multipath arrivals at 18 ms spacing were included, and they are easily identified for the 0 to 0.5 m/s Doppler velocities of the simulation, which used the 20dB ripple Chebyshev taper. Interestingly, the effect of the noise on the peak amplitudes overshadows the systematic decline in amplitude with increasing relative velocity. For a control, Figure 10 shows how random noise can slightly perturb the matched filter amplitudes with no relative motion.

18

REFERENCES

[1] P. F. Worcester, R. C. Spindel & B. M. Howe, "Reciprocal acoustic transmissions: Instrumentation for mesoscale monitoring of ocean currents," *IEEE J. Oceanic Eng.* 10 (1985), 123–137.

[2] S. W. Golomb, *Shift Register Sequences*, Holden-Day, San Francisco, 1967.

[3] B. M. Howe, J. M. Mercer, R. C. Spindel, P. F. Worcester, J. A. Hildebrand, W. S. Hodgkiss Jr., T. F. Duda & S. M. Flattè, "SLICE89: A single slice tomography experiment," in *NATO conference on ocean variability and acoustic propagation*, Kluwer, 1990.

[4] J. L. Spiesberger, R. C. Spindel & K. Metzger, "Stability and identification of ocean acoustic multipaths," *J. Acoust. Soc. Am.* 67 (1980), 2100–2017.

[5] J. J. G. McCue, "A note on the Hamming weighting of linear-FM pulses," *IEEE Proc.* 67 (1979), 1575–1577.

[6] F. J. Harris, "On the use of windows for harmonic analysis with the discrete Fourier transform," *IEEE Proc.* 66 (1978), 51–83.

[7] D. J. Thomson, "Spectrum estimation and harmonic analysis," *IEEE Proc.* 70 (1982), 1055–1096.

[8] J. N. Little & L. Shure, *Signal Processing Toolbox for Use with Matlab*, The MathWorks, Inc., Natick, MA, 1988.

[9] H. L. Van Trees, *Detection, Estimation, and Modulation Theory*, Pt. III, Wiley, New York, 1971.

DOCUMENT LIBRARY

March 11, 1991

Distribution List for Technical Report Exchange

Attn: Stella Sanchez-Wade
Documents Section
Scripps Institution of Oceanography
Library, Mail Code C-075C
La Jolla, CA 92093

Hancock Library of Biology &
   Oceanography
Alan Hancock Laboratory
University of Southern California
University Park
Los Angeles, CA 90089-0371

Gifts & Exchanges
Library
Bedford Institute of Oceanography
P.O. Box 1006
Dartmouth, NS, B2Y 4A2, CANADA

Office of the International
   Ice Patrol
c/o Coast Guard R & D Center
Avery Point
Groton, CT 06340

NOAA/EDIS Miami Library Center
4301 Rickenbacker Causeway
Miami, FL 33149

Library
Skidaway Institute of Oceanography
P.O. Box 13687
Savannah, GA 31416

Institute of Geophysics
University of Hawaii
Library Room 252
2525 Correa Road
Honolulu, HI 96822

Marine Resources Information Center
Building E38-320
MIT
Cambridge, MA 02139

Library
Lamont-Doherty Geological
   Observatory
Colombia University
Palisades, NY 10964

Library
Serials Department
Oregon State University
Corvallis, OR 97331-5503

Pell Marine Science Library
University of Rhode Island
Narragansett Bay Campus
Narragansett, RI 02882

Working Collection
Texas A&M University
Dept. of Oceanography
College Station, TX 77843

Library
Virginia Institute of Marine Science
Gloucester Point, VA 23062

Fisheries-Oceanography Library
151 Oceanography Teaching Bldg.
University of Washington
Seattle, WA 98195

Library
R.S.M.A.S.
University of Miami
4600 Rickenbacker Causeway
Miami, FL 33149

Maury Oceanographic Library
Naval Oceanographic Office
Stennis Space Center
NSTL, MS 39522-5001

Marine Sciences Collection
Mayaguez Campus Library
University of Puerto Rico
Mayagues, Puerto Rico 00708

Library
Institute of Oceanographic Sciences
Deacon Laboratory
Wormley, Godalming
Surrey GU8 5UB
UNITED KINGDOM

The Librarian
CSIRO Marine Laboratories
G.P.O. Box 1538
Hobart, Tasmania
AUSTRALIA 7001

Library
Proudman Oceanographic Laboratory
Bidston Observatory
Birkenhead
Merseyside L43 7 RA
UNITED KINGDOM

Mac 90-32

50272-101

REPORT DOCUMENTATION PAGE	1. REPORT NO. WHOI-91-13	2.	3. Recipient's Accession No.
4. Title and Subtitle Smoothly Modulated Frequency-Bounded Impulse Signals for Tomography			5. Report Date June 1991
			6.
7. Author(s) Timothy F. Duda and James F. Lynch			8. Performing Organization Rept. No. WHOI-91-13
9. Performing Organization Name and Address Woods Hole Oceanographic Institution Woods Hole, Massachusetts 02543			10. Project/Task/Work Unit No.
			11. Contract(C) or Grant(G) No. (C) N00014-87-K-0017 (G)
12. Sponsoring Organization Name and Address Office of Naval Research			13. Type of Report & Period Covered Technical Report
			14.

15. Supplementary Notes

This report should be cited as: Woods Hole Oceanog. Inst. Tech. Rept., WHOI-91-13.

16. Abstract (Limit: 200 words)

A group of amplitude and frequency modulated signals which generate narrow synthesized pulses and which also have smoothly varying phase are described. The frequency-sweep (chirp) signals have exactly-defined frequency content and differentiable phase. These signals can be used with efficient resonant transducers, if the resonant frequency is adjustable, and they have adequate Doppler response for use with drifting apparatus.

17. Document Analysis   a. Descriptors

pulse compression
tomography
signal processing

b. Identifiers/Open-Ended Terms

c. COSATI Field/Group

18. Availability Statement Approved for public release; distribution unlimited.	19. Security Class (This Report)	21. No. of Pages 22
	20. Security Class (This Page)	22. Price

(See ANSI-Z39.18)	See Instructions on Reverse	OPTIONAL FORM 272 (4-77) (Formerly NTIS-35) Department of Commerce